Efficient MRI simulation via integration of the signal equation over triangulated surfaces

L. Antiga[1], and D. A. Steinman[2]

[1]Mario Negri Institute for Pharmacological Research, Bergamo, Italy, [2]University of Toronto, Toronto, Ontario, Canada

Introduction

MRI simulation is an important tool for the design and optimization of pulse sequences and clinical protocols. Most MRI simulations, however, are restricted to geometrically simple objects or voxel-based descriptions of complex objects. Building upon the idea that the MRI signal equation can be integrated *analytically* over linear tetrahedral elements [1], we showed how *numerical* integration of the signal equation permits the use of volumetric elements that can conform more naturally to anatomically-realistic objects [2,3]. Here we extend and simplify these concepts further, by showing how the signal equation can be integrated over *surface* rather than volume elements.

Theory and Methods

The basic idea stems from the fact that, according to the Gauss (divergence) theorem, integration over a volume can be reduced to integration over the bounding surface, provided that integrand of the volume integral can be expressed as the divergence of a function. For the MRI signal equation, this can be accomplished provided the magnetization, *m*, is spatially uniform, in which case:

$$s(t) = \iiint_V m(\mathbf{x},t) e^{-2\pi i \mathbf{k}(t)\cdot\mathbf{x}(t)} dV = m(t) \iint_S \frac{i\mathbf{k}(t)\cdot\mathbf{n}(x)}{2\pi |\mathbf{k}(t)|^2} e^{-2\pi i \mathbf{k}(t)\cdot\mathbf{x}(t)} dS$$

where **n** is the unit vector normal to the surface. Relative to volumetric integration, efficiency is achieved in three ways. First, the cumbersome and often-difficult volumetric meshing step is avoided. Second, the number of elements over which integration is performed is reduced, on the order of the object's volume-to-surface-area ratio divided by the nominal element size. Third, for a given numerical integration order, fewer integration points are required for surface vs. volumetric elements.

To demonstrate the capabilities of this approach, we employed one of the segmented brain datasets from the OASIS repository [4]. Shown in Figure 1, the computational phantom was composed of CSF, white matter and grey matter surfaces (the skull surface was unavailable for privacy reasons), each of which was generated via Marching Cubes and then smoothed and decimated to ~200,000 linear triangles each. An axial acquisition was simulated using a 10-mm slice thickness, 175×207-mm^2 field-of-view, and a 64×72 matrix zero-padded to 128×144. The relative magnetizations were prescribed to produce a T1W image with CSF-suppression, and the slice profile was assumed to be ideal.

Results and Discussion

As shown in Figure 2, numerical integration of the surface triangulation produced a remarkably realistic-looking image of the brain. The simulation required about 3 minutes on a 2.13 GHz Macbook Pro, and storage requirements for the entire phantom were a modest 25Mb. Although these storage requirements are comparable to a voxelized phantom resolved to about 1 mm, it should be appreciated that the triangulated phantom resolves structures well below this level. To achieve a similar level of accuracy, a voxel-based phantom would require a substantial increase in resolution, bringing with it significant increases in storage and CPU requirements for the FFT-based MRI simulations.

Conclusions

We have presented an efficient MRI simulation technique that directly exploits the natural description of complex objects by surface triangulations. Although demonstrated here for objects possessing spatially-uniform tissue properties, this approach can be generalized to nonuniform tissue properties or magnetizations by decomposing $m(\mathbf{x},t)$ into complex exponential (i.e., Fourier) components.

References

[1] Truscott KJ and Buonocore MH. Simulation of tagged MR images with linear tetrahedral solid elements. JMRI 2001;14(3):336-40.
[2] Simedrea PS, Antiga L, Steinman DA. FE-MRI: Simulation of MRI using arbitrary finite elements. Proc ISMRM 14 (2006):2946.
[3] Simedrea PS. Numerical simulation of MRI using unstructured meshes. MESc Thesis, The University of Western Ontario (2006).
[4] http://www.oasis-brains.org/, MR session OAS1_0005_MR1. Accessed 27 October 2007.

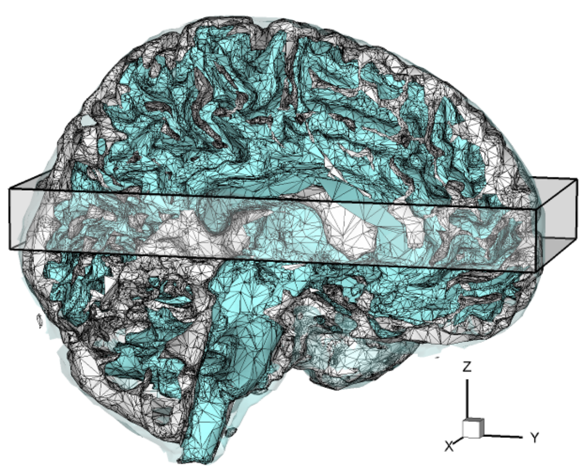

Figure 1 – Mid-sagittal view of the triangulated brain phantom.
The box indicates the location and thickness of the simulated image.

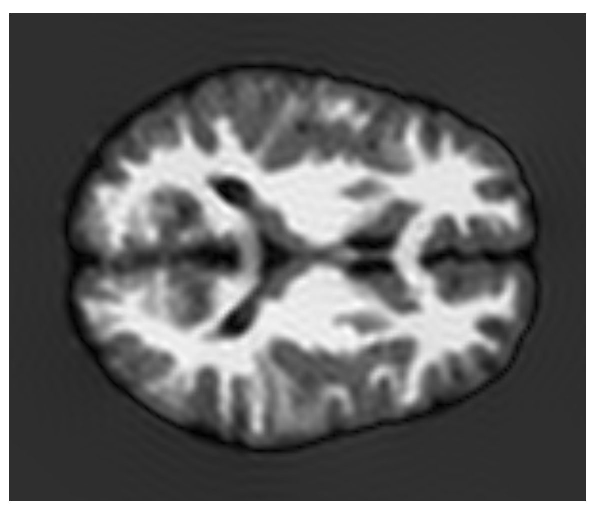

Figure 2 – Simulated axial T1W image of the brain